Simulation of an Optimized Poly 3-Hexylthiophene (P3HT) based solid state Dye Sensitized Solar Cell (ss-DSSC) using SCAPS

Kazeem Abdullahi Ojotu[1],Garba Babaji[2]

(Department of Physics Bayero University Kano, Nigeria)[1,2]

***ABSTRACT*:** *Solid state dye sensitized solar cells (ss-DSSCs) with conjugated organic polymer as hole transport material (HTM) have limited efficiencies due to the incomplete pore filling of the HTMs in the thick mesoporous photoanode and their low hole mobility. Herein, solar cell capacitance simulator (SCAPS) has been use to simulate ss-DSSC with Poly 3-Hexylthiophene (P3HT) as the HTM. The optimized photoanode thickness was found to be 1.3µm with an efficiency (η) of 4.90%, short circuit current density (Jsc) of 11.83mAcm^{-2}, open circuit voltage (Voc) of 734.2mV and fill factor (FF) of 56.45%. Beyond this optimum thickness, the efficiency of the cell decreases. This decrease is attributed to the increase in charge transport resistance for thicker TiO_2 photoanode which may also lead to recombination of charge carriers.*

KEYWORDS:*Optimization, P3HT, Photoanode, SCAPS, ss-Dssc*

I. INTRODUCTION

The demand for energy to cater for the ever increasing population of the world calls for greater concern. As predicted in the 2019 International Energy Outlook [1], fossil fuels (oil, coal and gas) will account for 78% of energy consumed in 2040. But unfortunately, fossil energy sources are limited and their consumption poses a high risk on the human populace. Owing to these demerits of its continuous use, there is need for finding an alternative clean, safer and renewable energy technologies.

A potential replacement for fossil fuels is the solar energy. A solar cell is a semiconductor device which converts solar energy from the suninto electrical energy[2].First generation silicon based solar cells are well established in terms of performance and production but their utilization is still low due to high cost of production. The second generationsof solar cells are flexible in application but accompanied with issues of complexity in fabrication, use of rare and toxic materials like In, Te and Cd and module stability [2]. The third generation of solar cells promises more flexibility, low cost and easy fabrication. Third generation solar cells are based on nanocrystals and nanoporous materials. This generation consist of dye sensitized solar cell (DSSCs), organic solar cells (OSC), quantum dot solar cells and perovskite solar cells (PSC). These are the novel technologies which are promising but yet to be commercially proven[2,3].

One of the most developed third generation solar cells arethe dye sensitized solar cells (DSSCs). This type of solar cells drew the interest of many research groups because of their low cost and easy method of fabrication [2-6]. A typical DSSC consist of three main components; dye-sensitized TiO_2 layer, hole transport mediator and counter electrode(C.E) [2]. Under illumination, electron-hole pairs occur in the dye molecules and electrons are then transferred to the conduction band of TiO_2 and leaving the hole behind in the oxidized dye molecules, the oxidized

dye is in turn regenerated by a hole transport mediator.

A solidstate dye sensitized solar cell is a kind of DSSC that a uses solid state hole transport material (HTM) as its hole transport mediator.Several types of p-type semiconductors such as ionic compounds [7, 8], small inorganic molecule [9] and conjugated organic polymers; [9-12] have been used as HTMs.

So far, efficiency of ss-DSSC is still on the low. This could be linked to factors like low charge mobilities of some HTMs, high surface defect density and poor pore filling capacity of HTMs in TiO_2 photoanode which collectively limit charge transport and increase trap assisted recombination.

A research group [9] fabricated a ss-DSSC using specifically-designed Poly 3-Hexylthiophene (P3HT) as the HTM. In their report, ss-DSSC based on P3HT shows a remarkable performance using a relatively thick TiO_2photoanode of 2μm [9]. However, earlier report had suggested that the efficiency of ss-DSSC can be improved by reducing the thickness of the photoanode [13,14]. ss-DSSC of TiO_2 photoanode thickness lesser than 2μm has been reported by previous literatures [15-17].The efficiency of ss-DSSC varies with the thickness of the TiO_2 photoanode as evident inthese previous literatures.

In this work, Solar Cell Capacitance Simulator (SCAPS) code was employed to investigate the performance of ss-DSSC withFTO/TiO_2&Dye/P3HT/Au structure. Specifically, the experimental work of Chevrier and co-workers [9] was simulated and the thickness of the TiO_2layer was optimized to produce the maximum efficiency.

Simulation reports helps to reduce the expenses which are incurred in fabrications, it gives more insight on the internal processes and also, it can be use to determine some parameters which may not be easily determined experimentally. The friendlier user interface coupled with variety of simulation techniques makes SCAPS a preferable choice for this work.

II. METHODOLOGY

2.1 Mathematical Model used by SCAPS

Simulation of ss-DSSC in this paper was conducted using SCAPS version 3.3.0.6. It is a onedimensional solar cell simulation program developed at the department of Electronics and Information Systems (ELIS) of the University of Gent, Belgium. The main functionality of SCAPS is to solve the one-dimensional semiconductor transport equations (equations 1-5) under steady state condition [18,19].

$$\frac{1}{q}\frac{dJ_n}{dx} = G_n - U_n \quad (1)$$

$$\frac{1}{q}\frac{dJ_p}{dx} = G_p - U_p \quad (2)$$

where J_n= electron current density, J_p= hole current density. $G_{n/p}$= generation rate of electrons and holes, $U_{n/p}$ = Recombination rate of electrons and holes.

SCAPS offer different kinds of recombination models; Shockley-Read-Hall (SRH), Auger recombination and Radiative recombination. In all these models, SRH model is the closest option to modeling recombination in DSSCs. SRH recombination is the dominant recombination mechanism in DSSCs and it starts when an electron is trapped by an energy state in the forbidden region [3].

The Poisson equation is given as

$$\frac{d^2\phi}{dx^2} = \frac{q}{\varepsilon_o \varepsilon_r}(p(x) - n(x) + N_d - N_a + \rho_{p-}\rho_n) \quad (3)$$

where ϕ(x), ε_o, ε_r, q, p(x), n(x), N_d, N_a, ρ_n *and* ρ_p are electrostatic potential, vacuum permittivity, relative permittivity, electric charge, hole concentration, electron concentration, charge impurities of donor, charge impurities of acceptor, electron distribution, and hole distribution respectively.

The drift and diffusion equations are

$$J_n = D_n \frac{dn}{dx} + \mu_n n \frac{d\varphi}{dx} \quad (4)$$

$$J_p = D_p \frac{dp}{dx} + \mu_p p \frac{d\varphi}{dx} \quad (5)$$

where D_n, D_p μ_n and μ_p are Diffusion coefficient of electrons, diffusion coefficient of holes, mobility of electrons and mobility holes respectively.

SCAPS solves these Basic semiconductor equations in 1-Dimension under steady state condition, it analyses the physics of the model and it explains the recombination profiles, electric field distribution, carrier transport mechanism and individual current densities [19].

The Efficiency of a solar cell is calculated using equation [20].

$$\eta = \frac{V_{oc} J_{sc} FF}{P_{in}} \quad (6)$$

where Voc, Jsc, FF and Pin are open circuit voltage, short circuit current density, fill factor and the input power of the solar cell respectively.

2.2 Simulation Procedure

Figure 1 briefly shows the general steps taking when using SCAPS, the first panel that appears after launching SCAPS is the "action panel"; the action panel contains sub sections such as "working point" and "action". To begin a new task, click set problem from the action panel and a new panel pops up displaying where layers properties will then be provided. The working simulation conditions are then stated in the "working point" section located in the action panel. The specified measurement (J-V, C-V, Q.E, or C-f) is then stated in the "Action" section located on the action panel. Finally, the simulation is carried out by clicking "Run". The output of the simulation is then displayed and can be saved by clicking "save".

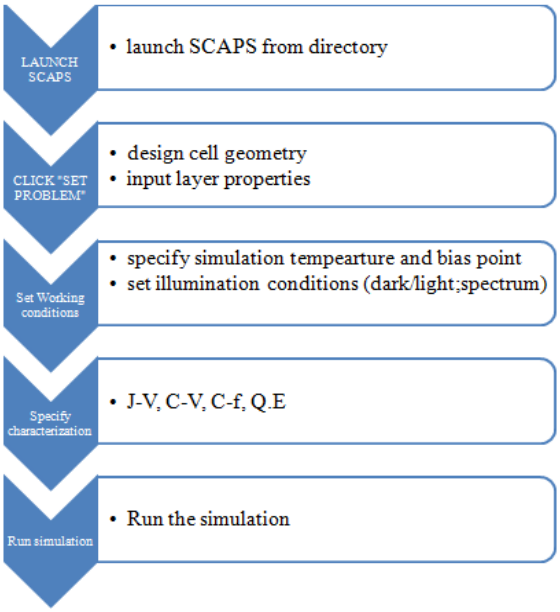

Figure 1: SCAPS general working procedure.

2.2.1 Simulation of Experimental Work

The performance of P3HT based ss-DSSC fabricated in the experimental work of [9]was simulated using SCAPS. The cell architecture is shown in Figure 2 and the input parameters used for simulationare shown in Table 1 and Table 2.

For the parameters not shown in Table 1, the following values were used for all layers: density of states in the conduction band and valence band are 2.2 x 10^{18}cm^{-3} and 1.9 x 10^{19}cm^{-3} respectively; thermal velocity of electrons and holes of 1 x 10^{7}cm/s; neutral defect (so that this defect leads to SRH recombination and not space charge) with a Gaussian distribution and characteristic energy of 0.1eV; and the capture cross section of electrons and holes of 2 x 10^{-14}cm^{2} [21]. The absorption profile of the layers was extracted from the experimental work in focus [9].

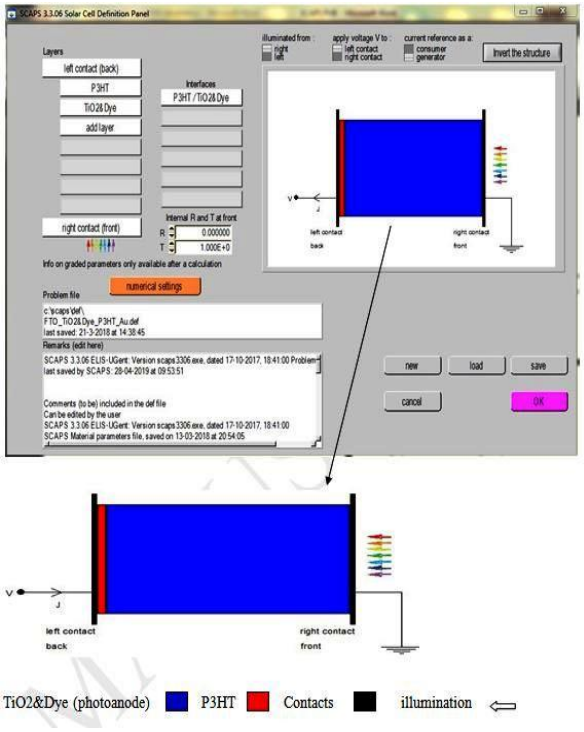

Figure 2: Cell definition panel in SCAPS showing the cell geometry: the front contact is fluorine doped tin oxide (FTO) while the back contact is gold (Au).

Table 1: Input parameter used in SCAPS for each Layers .

parameters	TiO_2&Dye Layer	P3HT Layer
L(μm)	2	0.08
Eg(eV)	3.2 [22]	2.1 [23]
χ (eV)	4.4 [24]	3.5 [23]
Ɛr	9.0 [25]	4.4 [26]
μ_e (cm^2/Vs)	2 [27]	4.8E-4 (Fitted)
μ_p (cm^2/Vs)	1 [27]	4.8E-3 (Fitted)
Nd (1/cm^3)	1.0 E +18	-

Na ($1/cm^3$)	-	1.0 E +17
Nt ($1/cm^3$ eV)	1.0E+10	1.0E+15 (Fitted)
I.F defect ($1/cm^2eV$)		1.69E+9 (Fitted)
Rs ($Ohms.cm^2$)	1.00 (Fitted)	
Rsh ($Ohms.cm^2$)	600 (Fitted)	

where L=thickness, Eg=energy band gap, χ= electron affinity Ɛr=relative permittivity, μ_e=electron mobility, μ_h=hole mobility, N_d= shallow donor density N_a= shallow acceptor density, N_t= layer defect density I.F= interface defect density, Rs= series resistance of substrate. Rsh= shunt resistance.

Table 2: Input parameters used as contact properties.

Contact	Type	Workfunction	Optical Properties
FTO	Front contact	4.4eV[28]	[29]
Au	Back contact	5.1eV [30]	[31]

To measure the accuracy of simulation results, calculation on error is also conducted based on percentage error (e_R), mean bias error (MBE) root mean square error (RMSE) and percentage mean absolute relative error (PMARE) using equations 7-10 respectively [32].

$$e_R = \frac{|R^{exp} - R^{sim}|}{R^{exp}} * 100\% \quad (7)$$

$$MBE = \frac{1}{N}\sum_{i=1}^{N}\left(R_i^{sim} - R_i^{exp}\right) \quad (8)$$

$$RMSE = \sqrt{\frac{1}{N}\sum_{i=1}^{N}\left(R_i^{sim} - R_i^{exp}\right)^2} \quad (9)$$

$$PMARE(\%) = \frac{100}{n}\sum_{i=1}^{n}\frac{Abs\left(R_i^{exp} - R_i^{sim}\right)}{R_i^{exp}} \quad (10)$$

2.2.2 TiO2 Photoanode Thickness Optimization

The TiO_2photoanode thickness was varied and the cell was characterized under Current density-Voltage (J-V) and Capacitance-frequency (C-f). The input parametersshown in Table 1and Table 2 were used.The working point conditions are 1 sun illumination (AM 1.5G) and at 300K.Additionally, frequency of simulation was swept from 100Hz to 10MHz during C-f simulation. Photovoltaic parameters were obtained from J-V characterization while information on charge resistive process was obtained from C-f simulation by analyzing the Nyquist plot of the cell using Multiple Electrochemical Impedance Spectra Parametization (MEISP) analyzer choosing Figure 3 as RC equivalent circuit of ss-DSSC [33].

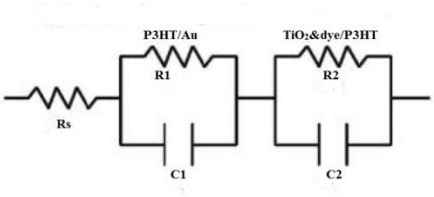

Figure 3: Equivalent circuit used in MEISP for extracting impedance parameters from Nyquist plot.

where Rs is an ohmic series resistance of the substrate, R1 and C1are the charge transport impedance at the P3HT/Au interface and R2 and

C2are the charge transport impedance at TiO_2&DYE/P3HT interface.

III. RESULTS AND DISCUSSIONS

3.1 Simulation of Experimental Work.

The photovoltaic parameters obtained by using SCAPs are shown in Table 3 with comparison to the experimental work [9]. Figure 4showsthe close agreement between the J-V curves obtained in our simulation and [9]. The simulated solar cell parameter; Voc, Jsc, FF and η have a percentage error of 1.39%, 0.09%, 3.45% and 1.46% respectively.

The MBE measures the average bias of the simulation. e_R measures the size of the error in percentage, RMSE measures the difference between the experimental and the simulated result while PMARE measures the mean absolute relative error between experimental findings and that of simulation.The MBE, RMSE and PMARE for the simulated result are 0.02, 0.04 and 1.58% respectively. These values are within the acceptable range when comparing experimental and simulation report[32].

This closeness justifies both the quality of the input parameters and the accuracy of using SCAPS to carry out simulation of this kind to a reasonable proximity with actual experimental expectations.

Table 3: Photovoltaic parameters obtained by SCAPS

Parameters	Simulation	Experimental[9]	e_R (%)
Voc(V)	0.73	0.72	1.39
Jsc (mA/cm^2)	11.38	11.37	0.09
FF	0.56	0.58	3.45
η (%)	4.71	4.78	1.46

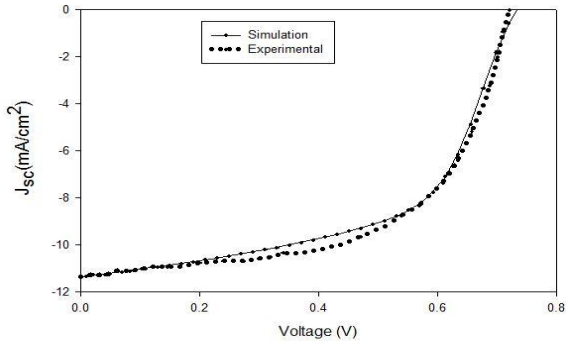

Figure 4: Illustrate the qualitative agreement between experimental and simulated J-V curves.

3.2 TiO_2 Photoanode Thickness Optimization for P3HT device.

Optimization of the TiO_2 photoanode thickness for P3HT cell configurationwas achieved by varyingthe thickness (L) of the photoanode as0.8μm, 1.1μm, 1.3μm, 1.5μm, 1.7μm, 2μm, 2.5μm and 3.0μm respectively. The result obtained for J-V and C-f characterizations is shown in Table 4 and Table 5 respectively.The efficiency of the cell increases as the thickness is increased from 0.8μm to 1.3μm.This could be as a result of increased in absorbed photons since this layer serves as the photoanode. Beyond 1.3μm, the efficiency of the cell decreases with increase in film thickness. The resistive parameter R2 shows reverse trend (Figure 5a). R2 increases beyond 1.3μm, higher value of R2 translates to higher resistance to charge transport which eventually affects charge mobility. This may account for decrease in cell efficiency beyond 1.3μm. The maximum efficiency is found to be 4.90% with Voc of 734mV, Jsc of 11.83$mAcm^{-2}$, FF of 56.45% and R2 of 22.70Ω.cm^2. From Table 6, the cell performance at photoanode thickness of 1.3μm shows an increase of 2.5% when compared with the cell performance for 2μm thickness initially reported in the literature [9].Thus, we conclude that the optimum thickness of TiO_2 photoanode is 1.3μm. This result is in line with earlier suggestions[7,16,17].

Table 4: Effect of TiO_2 Photoanode Thickness on Photovoltaic Parameters

L(μm)	V_{oc}(mV)	J_{sc}(mA.cm^{-2})	FF	η (%)
0.8	732.5	11.21	56.30	4.62
1.1	734	11.64	56.40	4.82
1.3	**734.2**	**11.83**	**56.45**	**4.90**
1.5	734.1	11.78	56.46	4.88
1.7	733.8	11.65	56.44	4.83
2	733.1	11.38	56.43	4.71
2.5	731.5	10.81	56.35	4.46
3	729.7	10.22	56.24	4.19

Table 5: Effect of TiO_2 Photoanode Thickness on Charge Transport Parameters

L(μm)	R2(Ω.cm^2)	C2(nF/cm^2)
0.8	22.94	89.80
1.1	22.86	89.79
1.3	**22.70**	**89.78**
1.5	22.86	89.79
1.7	22.93	89.80
2	23.11	89.81
2.5	23.63	89.84
3	23.70	89.86

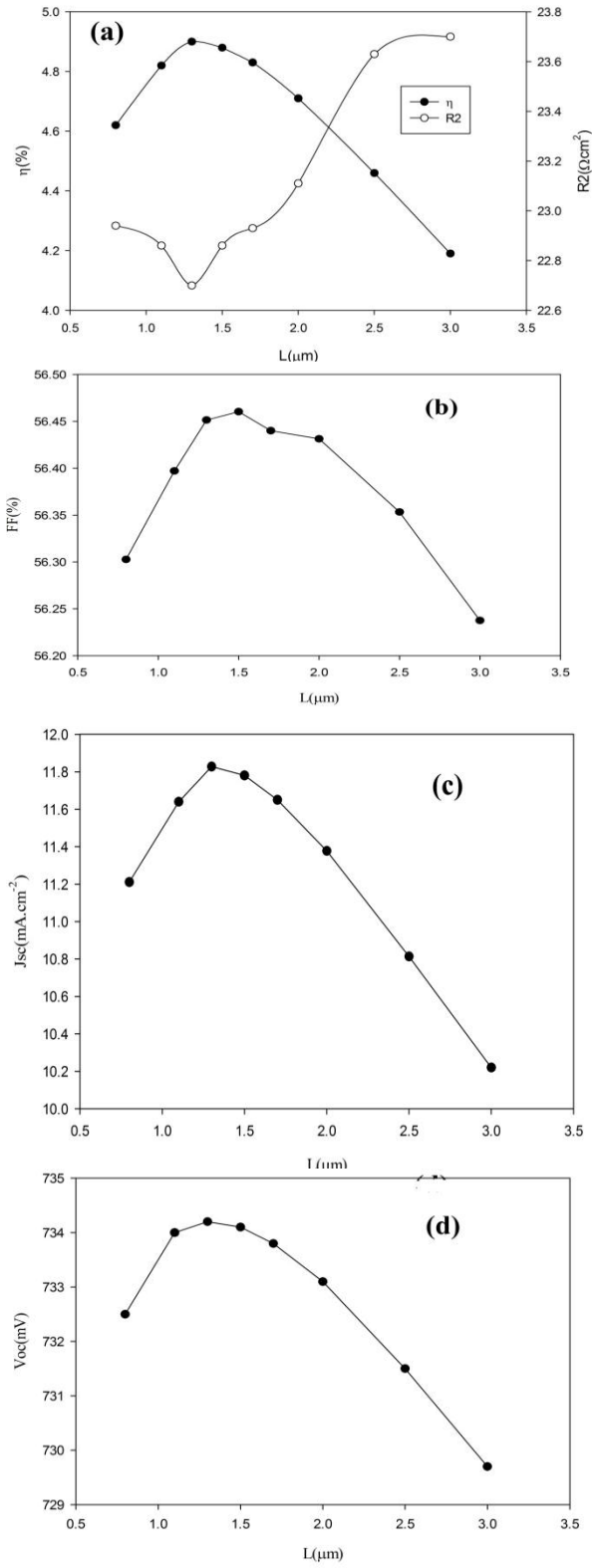

Figure 5: Effect of photoanode thickness on (a) Efficiency and R2 (b) fill factor (c) short circuit current density (d) open circuit voltage.

Table 6: Comparism of Solar Cell Parameters.

Reference	L (μm)	Voc (mV)	Jsc ($mAcm^{-2}$)	FF	η (%)
[16]	1	900	5.80	0.60	2.9
[15]	1	1003	6.30	0.60	3.85
[9]	2	720	11.37	0.58	4.78
[17]	0.08	672	12.7	0.56	4.53
This work	1.3	734	11.83	0.56	4.90

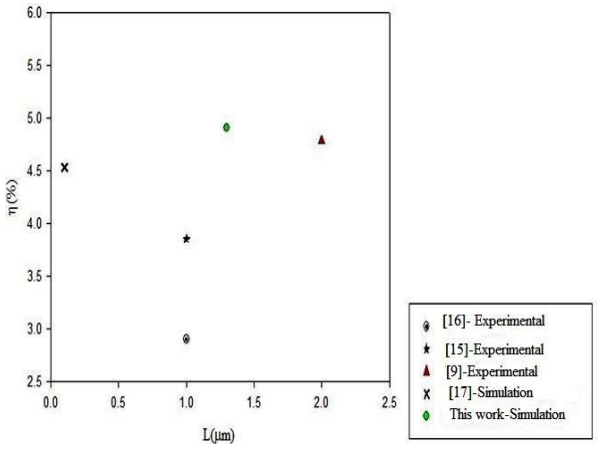

Figure 6: Correlation of Optimized Result with Previous Literature.

IV. CONCLUSION

The photoanode thickness of ss-DSSC is a very important factor to consider when fabricating ss-DSSC. Lower thickness will affect the capability of the cell to absorb more light while higher thickness may affects the ability of light to penetrate deep into the cell.Herein, we have investigated the optimum thickness of TiO_2 photoanode used in ss-DSSC via simulation. The efficiency of the cell increases from 4.62% to 4.90% as we increase the photoanode thickness from 0.8μm. to 1.3μm.Increasing photoanode thickness beyond 1.3μm leads to decrease in overall efficiency of the cell. Thicker photoelectrode will lead to higher resistance to charge transport across the cell which may further expose electrons to possible recombination with holes. This will affect the short circuit current, the fill factor and the open circuit voltage. From our analysis, we report the optimized thickness for FTO/TiO2&Dye/P3HT/Au device to be 1.3μm.

REFERENCES

[1] Conti J, Holtberg P, Diefenderfer J, LaRose A, Turnure J.T and Westfall L. (2019) "*International Energy Outlook 2016 with projections to 2040". United States: Energy Information Administration (EIA).* doi: 10.2172/1296780.

[2] Pathaakoti K., Manubolu M., and Hwary H. (2018) *Nanotechnological Applications for Environmental Industry (Chapter 48).In "Handbook of Nanomaterials for industrial Applications" Micro and Nano technologies page 894-907.*

[3] Mohammed N.M, Burhanudin Z.A, Oktiawati U.Y. (2014*) "Simulation of the effects of electrolyte concentration on Dye Solar Cell performance"5th International Conference on Intelligent and Advanced Systems (ICIAS).* DOI: 10.1109/ICIAS.2014.6869450.

[4] O'Regan B and Grätzel M. *"A low-cost, high-efficiency solar cell based on dye-sensitized colloidal TiO_2 films" Nature volume 353*, 1991, 737–740.

[5] Nazeeruddin M.K, Kay A., Rodicio I., Humphry-Baker R., Mueller E., Liska P., Vlachopoulos N, Grätzel M, (1993)*"Conversion of light to electricity by cis-X2bis(2,2'-bipyridyl-4,4'-dicarboxylate)ruthenium(II) charge-transfer sensitizers (X = Cl-, Br-, I-, CN-, and SCN-) on nanocrystalline titanium dioxide electrodes", Journal of America Chemical Society, vol.115* , 1993, 6382-6390.

[6] Hagfeldt, A. and Gratzel, M.. *"Light-Induced Redox Reactions in Nanocrystalline Systems"Chemical Reviews.vol95*, 1995, 49-68.

[7] Meng Q.B, Takahashi K., Zhang X.T, Sutanto I, Rao T.N, Sato O, and Fujishima A.*"Fabrication of an efficient solid-state dye-sensitizedsolar cell"Langmuir, 19,* 2003, 3572-3574

[8] Tennakone K., Kumara G., Kumarasinghe A.R, Wijayantha K.G.U, Sirimanne P.M. *" A dye-sensitized nano-porous solid-state photovoltaic cell "Semiconductor Science and Technology*. vol. 10, 1995, 1689.

[9] Chevrier M., Hawashinc H., Richetera S., Mehdia A., Surind M., Lazzaronid R., Duboisb P., Ratierc B., and Bouclécc J., Clément S. "Well-designed poly(3-hexylthiophene) as hole transporting material:A new opportunity for solid-state dye-sensitized solar cells." *Synthetic Metals* vol.226, 2017, 157–163.

[10] Yu Y. and Lira-Cantu M. "Solid state dye sensitized solar cells applying conducting organic polymers as hole conductors". *Physics Procedia , vol.8* , 2010, 22-27.

[11] Xu L., Wang J, Julia W. and Hsu P. *"Transport effects on capacitance-frequency analysis for defect characterization in organic photovoltaic devices"Physical Review Appliedvol. 6*, 2016, 064020.

[12] Zhang J.W, Vlachopoulos N, Jouinic M, Johansson M.B, Zhang X., Nazeeruddin M, Boschloo G., Johansson M.J, and Hagfeldt A. *"Efficient solid-state dye sensitized solar cells: The influence of dye molecular structures for the in-situ photo electrochemically polymerized PEDOT as hole transport material" Journal of Nano Energy, Volume 19*, 2016, 455-470.

[13] Snaith H.J, and Grätzel M. *"Electron and Hole Transport through Mesoporous TiO2 Infiltrated with Spiro-MeOTAD". Advance Material. vol. 19*,2007, 3643–3647.

[14] Wang M, Xu M, Shi D., RLi R., Cao F, Zhang G, Yi Z, Humphry-Baker R., Wang P, Zakeeruddin S.M, and Grätzel M, (2008) *"High-performance liquid and solid dye-sensitized solar cells based on a novel metal-free organic sensitizer"Advance Material, vol. 20* , 2008, 4460–4463.

[15] Zhang J.W., Zhu R., Li F., Wang Q., and Liu B. *"High-performance efficient solid-state organic dye-sensitized solar cells with P3HT as hole transporter." Journal of Physical Chemistry. Vol. C 115*, 2011 7038–7043.

[16] Kumar R.S.S, Grancini G, Petrozza A., Abrusci A., Snaith H.J. and Lanzani G. (2013) *"Effect of polymer morphology on P3HT-based solid-state dye sensitized solar cells: an ultrafast spectroscopic investigation"Optics Express* Vol. 21, No. S3.

[17] Mehrabian M and Dalir S. (2018) *"Numerical simulation of highly efficient dye sensitized solar cell by replacing the liquid electrolyte with a semiconductor solid layer"Optik - International Journal for Light and Electron Optics* Vol. 169. pp 214–223.

[18] Burgelman M, Decock K., Niemegeers A.I, Verschraegen J., and Degrave S. (2016) "*SCAPS manual*" Version: 29.

[19] Mandadapu U., Vedanayakam S. V, and Thyagarajan K.(2017) *"Simulation and Analysis of Lead based Perovskite Solar Cell using SCAPS-1D". Indian Journal of Science and Technology*,vol.10 issue 11, DOI: 10.17485/ijst/2017/v11i10/110721.

[20] Adamu B.I, Babaji G, Gidado A.S, Musa M , Abdullahi S.S and Hafeez H.Y (2015)*"Influence of Thickness on Titanium Dioxide - Roselle (Zobo) Dye Sensitized Solar Cell" Northwest University Science, Faculty of Science Annual International Conference*, pp:298-301.

[21] Minemoto T. and Murata M. (2014.) "Device modeling of Perovskite solar cells based on structural similarity with thin film inorganic semiconductor solar cells." *Journal of Applied Physics.* vol. 116, pp504-505.

[22] Pfeifer V, Erhart P, Li S, … and Klein A. (2013) "Energy Band Alignment between Anatase and Rutile TiO_2" *Journal of Physical Chemistry Letters.* Volume 4 (23), pp 4182–4187.

[23] Nolasco J.C., Cabre R., Ferre-Bourull J., Marsal L.F., Estrada M., and Pattares J *"Extraction of poly (3-hexylthiophene (P3HT) properties from dark current voltage characterization in a P3HT/n-crystalline-silicon solar cell"Journal of Applied Physicsvol. 107*, 2010, 044505.

[24] Shen H, Omelchenko S.T, Jacobs D.A … and Catchpole K.R. (2018) *"In situ recombination junction between p-Si and TiO2 enables high-efficiency monolithic perovskite/Si tandem cells"Science Advances*. 4(12), 2018, 9711.

[25] Stamate M.D (2003). *"On the dielectric properties of dcmagnetron TiO2 thin films" Applied Surface Science.vol. 218(1)*, pp 317-322.

[26] Cho Y. S and Frankklin R.R (2012) *"Conducting Polymer Material Characterization using High Frequency Planar Transmission Line Measurement" Transmission on Electrical and Electronic Materials vol. 13, No 5*, pp 237-240.

[27] Zhang Q., Dandeneau C.S., Zhou X. and Cao G. (2009) *"ZnO Nanostructures for Dye-Sensitized Solar Cells" Advance Materials. Volume 21, Issue 41.* Pages 4087-4108.

[28] Shang D.S, Shi L., Sun S.R, Shen B.G, Zhuge F., Li R.W. and zhao Y.G (2010) *"Improvement of Reproducible Resistance Switching in Polycrystalline tungsten oxide Films by in situ Oxygen Annealing" Applied Science Letters* 96. ,072103 doi: 10.1063/1.3300637.

[29] Sites J.(2003) *"Quantification of losses in thin film polycrystalline solar cells"Solar Energy Materials and Solar Cellsvol. 75,* 243-251.

[30] Liang L., Yu C., Li X., Nazeeruddin M.K. and Gao P. (2018). *"All That Glitters is Not Gold: Recent Progress of Alternative Counter Electrodes for Perovskite Solar Cells" Nano Energy. Volume 52,* Pages 211-238.

[31] Bass, M., and Van Stryland, E.W.(1994).*Handbook of Optics vol. 2 (2nd ed.), McGraw-Hill (1994) ISBN 0070479747.*

[32] Ali M.H and Abustan I. (2014) *"A new novel index for evaluating model performance"Journal of Natural Resources and Development.* vol. 04, pp 1-9.

[33] Xia J., Yuan C., and Yanagida S., (2010) *"Novel Counter Electrode V2O5/Al for Solid Dye-Sensitized Solar Cells"Journal of Applied Material and Interface* Vol. 2 NO. 7 pp: 2136–2139.